Two-dimensional *XY*-like amorphous $Co_{68}Fe_{24}Zr_8/Al_{70}Zr_{30}$ multilayers

Martina Ahlberg, Gabriella Andersson, and Björgvin Hjörvarsson
Department of Physics and Astronomy, Uppsala University, Box 516, SE-751 20 Uppsala, Sweden
(Received 8 February 2011; revised manuscript received 6 April 2011; published 17 June 2011)

We present an experimental realization of a magnetic two-dimensional *XY* system using amorphous materials. The classification of the dimensionality is based on the critical behavior of amorphous $Co_{68}Fe_{24}Zr_8(d)/Al_{70}O_{30}$ (20Å) multilayers, where $d = 11 - 16$Å. Analysis of the remanent magnetization, the magnetic isotherms, the initial susceptibility, and the magnetic correlation length shows that the magnetic phase transition can be described by the 2D *XY* model. The samples are not paramagnetic above the critical temperature but are characterized by local magnetic order manifested in the field and temperature dependence of the magnetization. Furthermore, an average spin-spin interaction length of 8.1 Å was estimated using the thickness dependence of the Curie temperature.

DOI: 10.1103/PhysRevB.83.224404 PACS number(s): 75.50.Kj, 75.70.Cn, 75.40.−s, 64.60.F−

I. INTRODUCTION

Theories and experiments on critical phenomena link together diverse fields such as low dimensional magnetism and turbulence.[1] While melting is an example of a first-order phase transition, magnetic ordering is the first and foremost modeling system for second order, or *continuous*, phase transitions. The critical behavior of magnetic systems can be divided into nine universality classes according to their spatial and spin degrees of freedom. Of those, only four show net magnetization in the thermodynamic limit. This limit is reached when the system is infinitely large in all spatial dimensions (3D) or infinitely large in two spatial dimensions while infinitely small in the third dimension (2D). The critical temperature (T_c) is defined as the temperature where the spontaneous magnetization disappears. Close to T_c, the thermodynamic properties can be described by power laws, for which each universality class has its own characteristic set of critical exponents.[2]

It was long believed that no spontaneous magnetization could exist in 2D *XY* systems, as described in the well-known Mermin-Wagner theorem.[3] However, Kosterlitz and Thouless showed that even though 2D *XY* systems do not have a net magnetization, they undergo a phase transition with binding/unbinding of vortices at a critical temperature, known as T_{KT}. This transition has a signature of criticality making it possible to characterize the 2D *XY* systems experimentally.[4,5] Both the Mermin-Wagner theorem and the KT theory are valid in the thermodynamic limit, but the sample size needed to suppress collinear magnetic order is of planetary length scales and thus finite size effects guarantee magnetization in any realizable experiment.[6]

The influence of magnetic and structural disorder on phase transitions has been the source of inspiration for a large amount of theoretical and experimental efforts.[7–11] One of the important findings is the confirmation of the Harris criterion,[12] which states that structural disorder will not affect the critical exponents if the exponent associated with the specific heat, α, is smaller than zero, i.e., when the specific heat does not diverge and therefore is finite for all temperatures. This is illustrated by bulk amorphous structures belonging to the 3D Heisenberg class where α is negative.

Studies of the critical behavior in thin amorphous magnetic layers are scarce and investigations of amorphous $(Tb_{0.27}Dy_{0.73})_{0.32}Fe_{0.68}$ multilayers are one of the few existing examples in the literature. Depending on the material in the spacer layers, Cr (magnetic) or Nb (non-magnetic), the dimensionality of these samples is either 3D Heisenberg or 2D Ising like.[13] These results show that the Harris criterion appears to be valid for the 2D Ising systems, with $\alpha = 0$. The exponent α is not defined in the 2D *XY* model and the Harris criterion can thus not be applied. However, theoretical work on a disordered 2D *XY* system shows that the phase transition survives if the disorder is small enough.[14,15]

The magnetic properties of amorphous thin films and multilayers are an emergent area of research, but the critical behavior is rarely addressed. To our knowledge, no measurements on layered 2D *XY* systems have been reported in the literature. This paper presents an experimental realization of structurally amorphous 2D *XY* magnetic layers.

II. EXPERIMENT

The multilayers were grown using magnetron sputtering. The nominal structure was $Si/SiO_2/Al_{70}Zr_{30}(20Å)/[Co_{68}Fe_{24}Zr_8(d)/Al_{70}Zr_{30}(20Å)] \times 10/Al_2O_3$ (20Å), where $d = 11 - 16$Å. The background pressure in the chamber prior to deposition was below 8×10^{-8} mTorr and the substrates were heated to 650°C for 1.5 h in order to outgas the Si surface. The films were deposited from alloy targets at room temperature and 2 mTorr argon (6N) was used as sputtering gas. The growth rates were kept low (≈0.4Å/s) to ensure good control of the layer thicknesses. The samples were grown using a previously developed procedure, which has been proven to yield high-quality amorphous structures.[16] The layering of the samples was investigated using x-ray reflectivity. The GenX package[17] was used to fit the data and the results of the fits for $d = 12 - 14$ Å are plotted in Fig. 1. The samples with magnetic layers thicker than 14 Å had a Curie temperature above 300 K, which is outside the accessible temperature range of the experimental setup used to measure the magnetization, and they are therefore not discussed further here. The final fitting parameter values for the other samples are listed in Table I. The samples are denoted after their nominal CoFeZr-thickness.

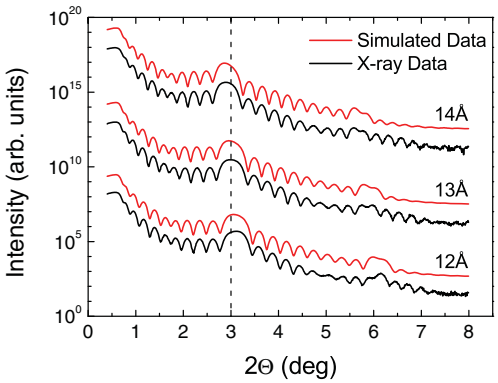

FIG. 1. (Color online) Measured x-ray reflectivity (black) together with simulations (red). Labels refer to the nominal CoFeZr thicknesses. The curves are offset for clarity and the vertical dashed line serves as a guide to the eye.

The magnetization was investigated using a setup which utilizes the magneto-optical Kerr effect (MOKE).[18] The samples were mounted in an optical cryostat, shielded by three layers of mu-metal to reduce magnetic stray fields. A 5 Hz alternating magnetic field (±7 mT) generated by a pair of Helmholtz coils was applied, and hysteresis loops were continuously recorded while varying the temperature with a cooling rate of 0.2 K/min. Measurements recorded during 30 seconds were averaged to give one final hysteresis loop. From this series of hysteresis loops, the remanent magnetization as a function of temperature was extracted. The resulting magnetization data are therefore a running average from a temperature range of 0.1 K, which ultimately determines the temperature resolution in the analysis. In addition, the ac susceptibilities of the samples were measured using the same setup. The excitation field was then about 20μT and the frequency 215 Hz.

III. THEORETICAL BACKGROUND

The spontaneous magnetization vanishes at the critical temperature (T_c). In the vicinity of T_c, some of the magnetic properties can be described by the following power laws[2]:

$$M(T) \propto (1 - T/T_c)^{\beta} = (-t)^{\beta}, \quad (1)$$

$$M(H) \propto H^{1/\delta}, \quad (2)$$

$$\chi(T) \propto (T/T_c - 1)^{-\gamma} = t^{-\gamma}, \quad (3)$$

$$\xi \propto (T/T_c - 1)^{-\nu} = t^{-\nu}, \quad (4)$$

where M is the zero-field magnetization, T is the temperature, H is the applied field, χ is the magnetic susceptibility, ξ is the magnetic correlation length, and t is the reduced temperature.

TABLE I. Result of the fits to the XRR data, where Λ is the bilayer thickness, d_{CoFeZr} is the thickness of the CoFeZr layers, and σ_r is the average roughness in the CoFeZr layers.

Sample	Λ (Å)	d_{CoFeZr} (Å)	σ_r (Å)
11 Å	27.70(9)	10.9(5)	5.0(7)
12 Å	29.11(6)	11.9(3)	5.1(1)
13 Å	30.04(6)	13.0(9)	5.2(2)
14 Å	31.16(6)	14.3(2)	5.1(2)

The critical exponent β was determined to be $3\pi^2/128 \approx 0.23$ for the finite size 2D *XY* phase transition, by Bramwell and Holdsworth in 1993.[6] In this and following papers, they successfully built up the theory of finite size 2D *XY* systems, which in many aspects is identical to the KT theory and all properties converge to those of a KT-phase transition in the thermodynamic limit.[6] In contrast to other phase transitions, finite size 2D *XY* systems are not characterized by *one* critical temperature but three, the Curie temperature (T_C), the Kosterlitz-Thouless temperature (T_{KT}), and the finite-size shifted KT-temperature (T^*). T_C is the usual critical temperature, where the long-range spontaneous magnetization disappears, but finite-size effects give substantial contribution to the magnetization making it hard to unambiguously determine its value. In the thermodynamic limit, the critical exponents δ and η take their universal values of 15 and 1/4, respectively, at T_{KT},[5] but in finite systems the universal values appear at another temperature T^*:[19]

$$T^*(L) \cong T_{KT} + \frac{\pi^2}{4c(\ln L)^2}, \quad (5)$$

where L is the system size and $c \approx 2.1$ is a constant. T_{KT} is still important and plays a role when characterizing the correlation length and the susceptibility:[5,20]

$$\chi(T) \propto \xi^{2-\eta} \propto \exp\left[\frac{(2-\eta)b}{(T/T_{KT} - 1)^{1/2}}\right] = \exp\left(\frac{B}{\epsilon^{1/2}}\right), \quad (6)$$

where b is a nonuniversal constant.[21]

The above equation implies that Eqs. (3) and (4) are not valid for 2D *XY* systems and therefore γ and ν are not defined.

IV. RESULTS AND DISCUSSION

A. Critical properties

T_C and β were determined by fitting the temperature dependence of the remanent magnetization, using Eq. (1), for all the samples exhibiting spontaneous magnetization. The 11 Å sample showed no ferromagnetic ordering for $T > 15$ K and the samples with magnetic layers thicker than 14 Å had a $T_C > 300$ K. The critical temperatures of these samples are outside the accessible temperature range of the experimental setup and are therefore not discussed further. The result obtained from the 12 Å sample is shown in Fig. 2, which also illustrates hysteresis loops obtained at different temperatures. The magnetization does not go abruptly to zero but shows a pronounced tail. The Curie temperature obtained from this fit was used as an input for a double logarithmic plot of the magnetization data versus reduced temperature; see Fig. 3. The resulting linear fit in the interval $10^{-3} \leqslant -t \leqslant 10^{-1}$ is also shown in the figure.

The presence of inhomogeneities in the sample can potentially give rise to a distribution in the inherent ordering temperature and thereby a tailing in the magnetization. A routine proposed by Elmers *et al.*,[22] which involves a convolution of Eq. (1) and a Gaussian distribution of T_C, was used in an attempt to capture this. The convolution yielded decreased range of linearization and was therefore abandoned. The tailing can therefore be ascribed to finite size effects, which are hard to capture quantitatively. The results of the

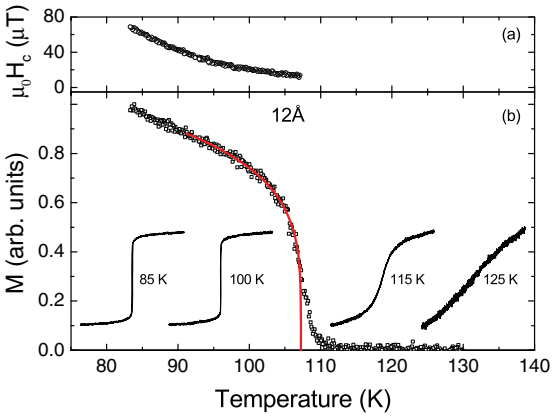

FIG. 2. (Color online) (a) The coercive field of the 12 Å sample versus temperature. (b) Magnetization of the 12 Å sample versus temperature. The solid line (red) corresponds to a fit to Eq. (1). The insets show hysteresis curves, where the applied field is $-6.5 \leqslant \mu_0 H \leqslant 6.5$ mT, at selected temperatures.

direct fits are presented in Table II and the linear fits are plotted in Fig. 3. Only the 12 Å sample has the β value expected for the 2D XY class, but all samples are closer to $\beta = 0.23$ than to a value associated with any other universality class. No trend in β with increasing film thickness that could indicate a cross-over to 2D Ising or 3D critical behavior can be observed. A deviation from the expected 2D XY value of β can be understood within the framework of the 2D XYh_4 model. 2D XYh_4 systems exhibit a bimodal distribution in β, bound by the values for the pure 2D Ising and XY classes, depending on the strength of the four-fold crystal field (h_4) relative the coupling constant (J).[23] Here, the h_4 field must be regarded as a local property[16] due to the absence of a global anisotropy, but the effect on the phase transition stays the same. The observation of β being lower than 0.23 can therefore be viewed as a consequence of the presence of a local random anisotropy originating in the spin orbit coupling.[16]

The critical exponent δ was determined in a similar fashion as β: all $\log(M)$ versus $\log(\mu_0 H)$ were fitted to linear expressions and δ at T_C was extracted. Equation (2) fails to describe the magnetization at low fields due to the coercivity (H_c). Hence, only fields between 0.1 and 6.5 mT were included

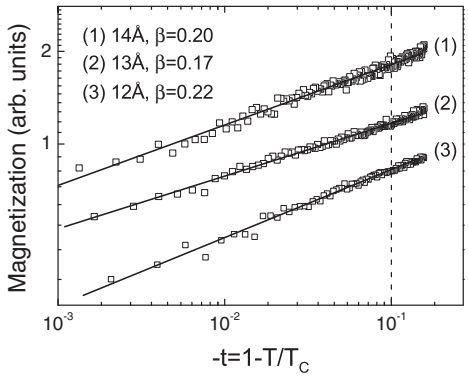

FIG. 3. Magnetization versus reduced temperature plotted on a logarithmic scale. β was determined by a linear fit (solid line) of the data in the interval $10^{-3} \leqslant -t \leqslant 10^{-1}$, indicated by the dashed line. The data sets are offset for clarity.

TABLE II. Critical properties determined from the remanent and field dependent magnetization. T_C and β were obtained from a direct fit to Eq. (1).

Sample	T_C (K)	T^* (K)	T_{KT} (K)	$\delta@T_C$	β
11 Å	< 15	–	–	–	–
12 Å	107.22(3)	101.0(1)	98.96(1)	7.9(2)	0.22(1)
13 Å	168.3(1)	163.9(1)	162.5(1)	8.9(2)	0.17(1)
14 Å	225.5(1)	220.1(1)	218.3(1)	8.7(2)	0.20(1)
>14 Å	>300	–	–	–	–

in the fits, to stay above $\mu_0 H_c$ in the temperature range of interest. The magnetization as a function of applied field is plotted on a double-logarithmic scale in Fig. 4 and δ at $T = T_c$ is presented in Table II.

It is evident that the δ exponents belong neither to the 2D Ising ($\delta = 15$[24]) nor to the 3D classes ($\delta \approx 4.78$[25]). This is in agreement with the 2D XY model, where δ is not defined at T_C. Instead, T^* can be identified as the temperature where $\delta = 15$; see Fig 5.

According to Bramwell and Holdsworth,[6] there is a simple relationship between T_C, T^*, and T_{KT},

$$T_C - T_{KT} = 4(T^* - T_{KT}), \tag{7}$$

and thus the knowledge of T_C and T^* can be used to calculate T_{KT}. The result of the analysis of the magnetization is presented in Table II.

The ac susceptibilities of the 12–14 Å samples are plotted in Fig. 6. They show a remarkable change of shape with thickness, but the common feature is that the peak corresponding to the phase transition is followed by a second broad feature at lower temperatures.

Two peaks in the ac susceptibility have been observed for amorphous bulk samples when measured in a weak external dc field.[26–29] The samples in those studies (besides that of Gaunt *et al.*[28]), exhibit a mixed spin glass and ferromagnetic phase with $T_C \approx T_{FG}$, i.e., the ferromagnetic to spin-glass transition temperature. Gaunt *et al.* argued that the second peak was an effect of details in the magnetization process such as domains,[28] and Saito *et al.* used a similar approach to explain a third peak they observed between the peaks corresponding to T_C and T_{FG}.[26]

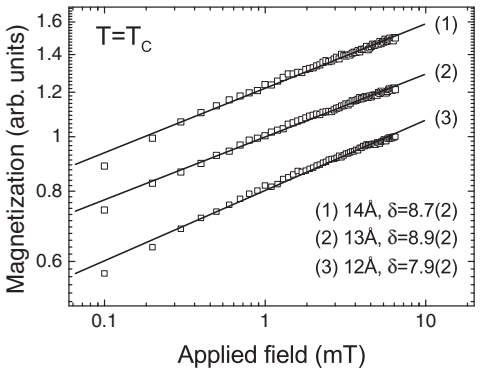

FIG. 4. Magnetization versus field at T_C plotted on a logarithmic scale. δ was determined by a linear fit (solid line) to the data. The data sets are offset for clarity.

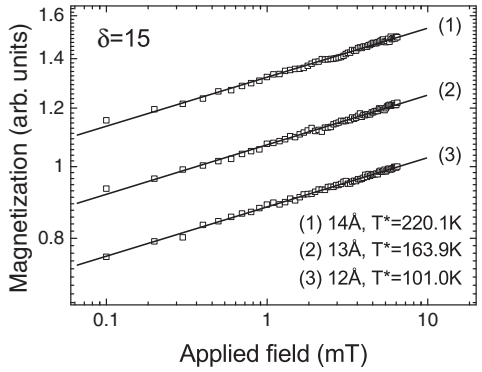

FIG. 5. Magnetization versus field at the temperature defined as T^*, where $\delta = 15$, plotted on a logarithmic scale. The data sets are offset for clarity.

In those examples, no additional peaks are visible without an external dc field on the order of 2 mT, but in the present measurements on the CoFeZr multilayers, no static field is applied and, furthermore, the samples were shielded from the Earth's magnetic field. In addition, no maximum in the magnetization is observed for temperatures around the second peak, which is expected if the sample has spin-glass character. At low temperatures, the remanent magnetization decreases, but this reduction is a consequence of the field being too weak to saturate the magnetization, and consequently minor loops are recorded. The results given by Sankar *et al.*[30] are closer to the one reported here, even though the measurements are on polycrystalline bulk samples, and the authors observe a splitting of the ac susceptibility without applying any external dc fields. Their samples are close to the spin-glass composition, and they refer the second peak to interaction between large long-range ordered ferromagnetic clusters and small magnetically ordered clusters. They do not give an explicit statement on what kind of magnetic ordering is present in the small clusters, i.e., if they are ferromagnetic, spin-glass like, or show some other ordering.

The shape of the susceptibility of the CoFeZr samples can be regarded as being caused by two mechanisms. The peak at high temperatures corresponds to the ordering of spins on large length scales, i.e., the phase transition. But not all spins are ordered at and right below T_C, some are still uncorrelated and the ordered regions can have different easy axes due to the presence of random anisotropy in the samples. When the ferromagnetic regions grow and meet, the spins on their boundaries become frustrated and follow the applied field easily. This effect could give rise to a second peak as observed here. Another view, which originates from the inherent properties of the 2D *XY* model, can be more appropriate. 3D samples exhibit a well-defined critical temperature, while 2D *XY* samples exhibit criticality in a wide temperature range. The consequence of the criticality is nonvanishing susceptibility, originating in the quasi-static magnetic excitations caused by the presence of vortex states. The susceptibility of a finite two-dimensional *XY* model has been calculated and it shows indeed a double divergence.[31]

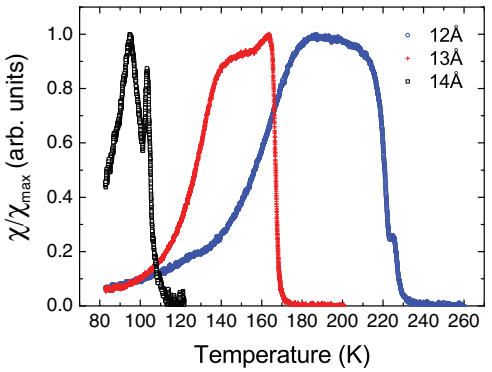

FIG. 6. (Color online) The real part of the ac susceptibility, from left to right the 12 Å, 13 Å, and 14 Å sample. The data is normalized to the maximum value of the susceptibility for each sample.

The analysis of the critical properties above implies that the samples with $d = 12 - 14$ Å belong to the 2D *XY* class and therefore the initial susceptibility should show an exponential divergence [Eq. (6)]. B is determined by a least-square linear fit to $\ln(\chi)$ versus $\epsilon^{-1/2}$. Taking the logarithm of χ naturally leads to the need to cut the data where $\chi = 0$. The unknown parameters in the fits are not only B and a constant, but also the starting point (T_x), which gives the best fit. To be able to find this point, the goodness of the fit is maximized by minimizing the reduced χ^2 value which is given by

$$\chi^2 = \frac{1}{n-2} \sum_{i_{T_{\max}}}^{i_{T_x}} \frac{1}{\sigma_i} \left[\chi_i - \exp\left(\frac{B}{(T_i/T_{\mathrm{KT}} - 1)} + a \right) \right]^2, \quad (8)$$

where χ_i is the ith data point in the susceptibility, $T_{\max}$ is the maximum value of the temperature, T_x is the starting point of the fit, σ_i is the uncertainty associated with the data, B and a are the constants determined by the linear fit, and n is the number of data points included in the fit. Note that not only the data points of the linear fit are included in the calculation of χ^2 but also the data where $\chi \leqslant 0$. In the procedure, T_{KT} was changed in steps of 0.02 K and for each value of T_{KT}, T_x was varied. A new linear fit was made to the data for each combination of T_{KT} and T_x. The fit with the best χ^2 was found and used for the final results, which are given in Table III. For completeness, a power-law divergence [Eq. (3)] was used to describe the susceptibility. The exponent γ was determined using a scheme analogous to the one described above for the constant B.

Figure 7 shows a comparison between the power-law fit and the exponential fit for the 13 Å sample. Both equations give a good fit to the data, but the γ values do not agree with the expected ones for the 2D Ising or 3D models ($\gamma = 1.75$[24] and $\gamma = 1.24 - 1.40$,[25,32] respectively). In addition, the fitted

TABLE III. Result of linear fits of Eqs. (3) and (6) to the initial susceptibilities. The fits were made using both the critical temperatures from the analysis of the magnetization data (†) and the critical temperature as a free parameter (††).

Sample	γ †	γ ††	T_C (K) ††	B †	B ††	T_{KT} (K) ††
12 Å	0.90(40)	1.52(4)	102.7	1.72(5)	2.09(6)	98.0
13 Å	1.07(9)	2.65(5)	165.2	1.82(3)	1.72(3)	162.7
14 Å	1.46(7)	2.78(6)	221.7	1.81(4)	2.03(4)	217.6

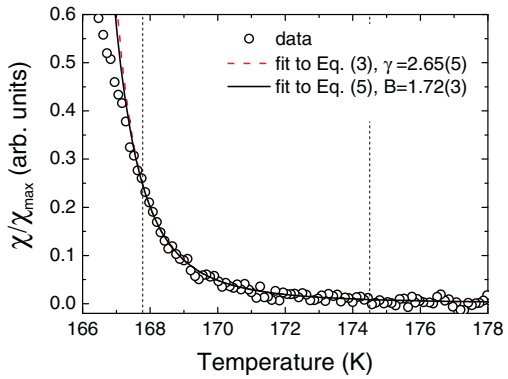

FIG. 7. (Color online) Linear fit to the initial susceptibility of the 13 Å sample to Eq. (6) (red dashed line) and Eq. (3) (black solid line); see text for details. The data points included in the fit are indicated by the dashed vertical lines.

values of T_{KT} are much closer to the ones determined from the magnetization data than the values of T_C. The constant B is a nonuniversal value, but it can be noted that the values obtained here are close to that of an earlier measurement on thin films where $B = 1.6 \pm 0.1$.[22] The susceptibility data of the 12 Å sample were very scattered and the results of those fits must be interpreted with caution.

Both T_C and T^* increase linearly with the thickness of the CoFeZr layers; see Fig. 8. A linear dependence of T_C on thickness is also found for thin films in the few monolayer limit.[33,34] Zhang and Willis used a model within the mean-field approximation to derive an equation that links the shift of the Curie temperature $[T_C(n)]$ to the average spin-spin interaction range (N_0):

$$\frac{T_C(n)}{T_C(\infty)} = (n-1)\frac{1}{2N_0}, \tag{9}$$

where n is the thickness of the ultrathin film in monolayers (ML) and $T_C(\infty)$ is the bulk Curie temperature. The equation implies that a 1 ML film will not be ferromagnetic, which is incorrect in many cases. The equation nevertheless gives a good approximation of N_0 that is in reasonable agreement with experimental data.[35]

The spin-spin interaction length in the CoFeZr layers can be estimated using the same approach. The Curie temperature of bulk $Co_{68}Fe_{24}Zr_8$ is not known but is roughly 800 K.[36,37] Since the observed upper thickness limit for magnetic ordering is 11 Å, Eq. (9) needs to be slightly modified:

$$\frac{T_C(d)}{T_C(\infty)} = (d-d_0)\frac{1}{2N_0}, \tag{10}$$

where d denotes the thickness of the magnetic layers in Ångströms and d_0 is the thickness where no magnetic order appears at $T > 0$. A fit of Eq. (10) to the data gives $N_0 = 8.1$ Å, which is about the same range as in the itinerant ferromagnets Co and Ni: $N_0^{Co} \approx 3.9$ Å, $N_0^{Ni} \approx 8.8$ Å.[35]

The Curie temperature of an 11 Å thick layer is overestimated if a linear relationship between T_C and d is assumed for all thicknesses. This is equivalent to crystalline thin films, where $T_C(d)$ follows a power law for large d[38] and is then linear for smaller d values with a change of slope for thicknesses close to d_0.[39]

B. Field dependence above T_c

All long-range magnetic order is destroyed as the temperature exceeds the Curie temperature. This does, however, not imply the absence of short-range order and the correlation length (ξ) can be used as a measure of the range of the short-range order. In the 2D *XY* model, the correlation length decays as[5,20]

$$\xi(T) \propto \exp\left[\frac{b}{(T/T_{KT}-1)^{1/2}}\right], \tag{11}$$

where b is a constant. The magnetic correlation length cannot be directly measured from the experimental techniques used here. The presence of magnetic correlation can, however, be obtained by exploring the field dependence of the magnetization above T_C, using the following assumptions: Assume that the fluctuations can be regarded as local order in the form of *dynamic macrospins* and that the size of these is only marginally affected by small external fields. As seen in Fig. 9, the hysteresis loop (12 Å at T =114K, $t = 0.06$) does not exhibit a typical linear paramagnetic behavior, but an *s* shape. The linear response of the magnetization at small fields can be understood as the lining up of the otherwise uncorrelated macrospins. At higher fields, the macrospins are already aligned, giving rise to much weaker field dependence.

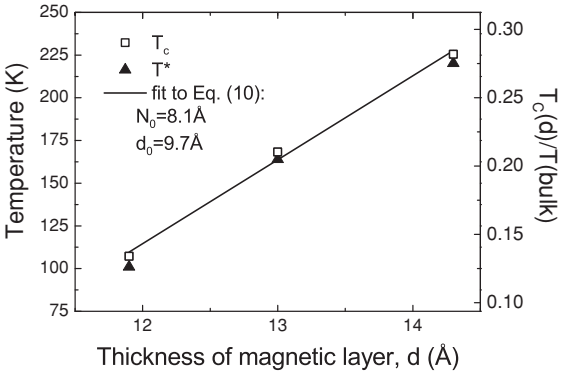

FIG. 8. T_C (open squares) and T^* (closed triangles) versus the thickness of the magnetic layer. The right axis shows the relative Curie temperature and the solid line is a fit of Eq. (9) to T_C.

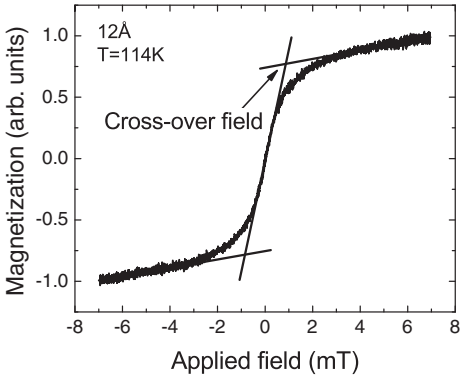

FIG. 9. The hysteresis loop at 114K of the 12 Å sample. The intersection of two linear fits to the magnetization at low and high applied field defines the cross-over field.

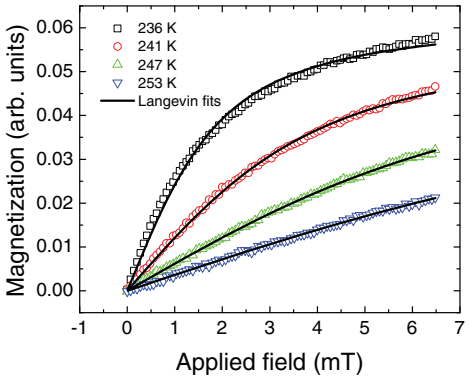

FIG. 10. (Color online) The top half of hysteresis loops of the 14 Å sample at four different temperatures. The solid lines (red) correspond to fits to Eq. (12).

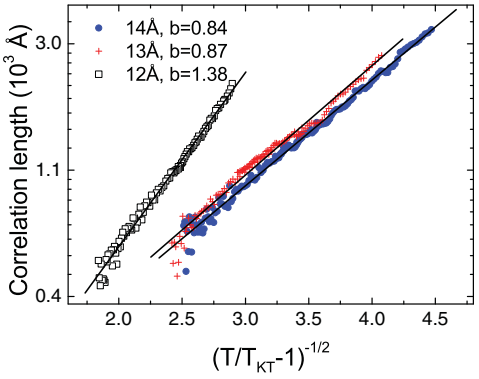

FIG. 12. (Color online) The correlation length as function of $(T/T_{KT}-1)^{-1/2}$ on a semi-logarithmic scale. The constant b was determined by linear fits (black lines) to Eq. (11).

Here we define the *cross-over field* (COF) by the intersection of two lines connecting these two field regions. The COF should therefore be a measure of the field needed to align the macrospins, which in turn should scale inversely proportional to their magnetic moment.

The COF data only give a qualitative estimate of the magnetic moment of the macrospins. However, it can be put on a more rigorous footing using a macrospin model where $M(H)$ can be described as

$$M(H) \propto n\mu \mathrm{L}\left(\frac{\mu_0 H \mu}{k_\mathrm{B} T}\right). \tag{12}$$

Here, n is the density of macrospins, μ is the magnetic moment, μ_0 is the permeability of free space, k_B is Boltzmann's constant, and $\mathrm{L}(x) = 1/\tanh(x) - 1/x$ is the Langevin function.[40]

The model allows an estimation of the average magnetic moment in the ordered regions by fitting the hysteresis loops to Eq. (12). Only the top half of each loop was used in the analysis, and in Fig. 10, examples from four temperatures are plotted. Figure 11 shows the clear correspondence between the COF and Langevin approaches.

The magnetic moment is proportional to the number of spins in the volume of the macrospin, and the correlation length can be calculated if a cylindrical shape of the macrospin is assumed:

$$\xi \propto \left(\frac{V}{d}\right)^{1/2} \propto \left(\frac{M}{md}\right)^{1/2}, \tag{13}$$

where V is the volume of the macrospins, d is the thickness of the magnetic layer, M is the average magnetic moment of the macrospins, and m is the moment per magnetic atom.

The moment per atom can be estimated, using a literature value of the remanent magnetic moment at $T/T_\mathrm{C} \approx 0.4$ of bulk CoFeZr (49 emu/g[37]), which corresponds to 0.58 μ_B/atom in the CoFeZr layers in the samples. The size of both the magnetic moment per macrospin and the correlation length should be taken as indicative values, due to the inherent uncertainties in these estimations.

The constant b was determined by linear fits of the correlation length plotted on a semi-logarithmic scale. The results are presented in Fig. 12. The constant B, which is associated with the susceptibility, is equal to $(2-\eta)b$ according to Eq. (6). The behavior of η above T_C is not well established so the approach of Als-Nielsen *et al.*[20] was used, where $\eta = 0$ and thus $B = 2b$. The 13 Å and 14 Å samples fulfill this relationship, while the 12 Å sample does not. The B value of the latter is questionable though, due to the poor susceptibility data. If the correlation length is plotted versus the reduced temperature on a double logarithmic scale as a function of the reduced temperature, the data appear linear with a slope of ≈ -0.85 for all samples.

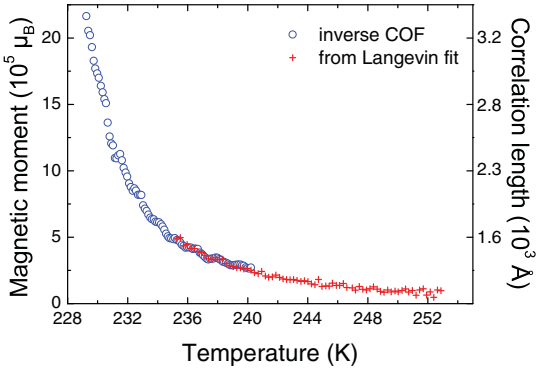

FIG. 11. (Color online) Comparison between the inverse cross-over field and the magnetic moment from Langevin fits of the 14 Å sample. The COF data is rescaled with respect to the Langevin data at 237 K.

V. CONCLUSIONS

All available magnetic properties have been explored in a thorough investigation of the critical behavior of thin amorphous $Co_{68}Fe_{24}Zr_8$ layers. Analyses of the remanent magnetization, the magnetic isotherms, the initial ac susceptibility, and the magnetic correlation length show that the samples are best described by the two-dimensional XY model. These layers therefore represent an experimental realization of a 2D XY system with structural disorder. Furthermore, the field and temperature dependence of the magnetization above the Curie temperature has been used to obtain a measure of the correlation length using the magneto-optical Kerr effect.

Structural disorder and random anisotropy are found not to destroy the 2D XY transition. The only exponent that can be compared to theory is β, which is somewhat smaller than the expected theoretical value for the pure 2D XY model. This can be viewed as a consequence of the presence of a local anisotropy, a perturbation shifting the universality toward the 2D XYh_4 class. The average spin-spin interaction range in the $Co_{68}Fe_{24}Zr_8$ layers has been estimated to 8.1 Å from the variation of critical temperatures with layer thickness.

The susceptibility shows two peaks. The peak at high temperature marks the phase transition to long-range ferromagnetic ordering. The wider peak at lower temperature may originate from frustrated spins which easily follow the applied field. An alternative interpretation is that this second peak is an inherent effect of the extended criticality in 2D XY samples.

These results make a strong contribution to the accumulated shared knowledge of the magnetic properties of amorphous materials.

ACKNOWLEDGMENTS

Financial support from the Swedish Research Council (Vetenskapsrådet) and the Knut and Alice Wallenberg Foundation is gratefully acknowledged.

[1] S. T. Bramwell, P. C. W. Holdsworth, and J.-F. Pinton, Nature (London) **396**, 552 (1998).
[2] H. E. Stanley, *Introduction to Phase Transitions and Critical Phenomena* (Oxford University Press, Oxford, 1993).
[3] N. D. Mermin and H. Wagner, Phys. Rev. Lett. **17**, 1133 (1966).
[4] J. M. Kosterlitz and D. J. Thouless, J. Phys. C **6**, 1181 (1973).
[5] J. M. Kosterlitz, J. Phys. C **7**, 1046 (1974).
[6] S. T. Bramwell and P. C. W. Holdsworth, J. Phys. Condens. Matter **5**, L53 (1993).
[7] S. N. Kaul, J. Magn. Magn. Mater. **53**, 5 (1985).
[8] R. Reisser, M. Fähnle, and H. Kronmüller, J. Magn. Magn. Mater. **75**, 45 (1988).
[9] A. Perumal, V. Srinivas, V. V. Rao, and R. A. Dunlap, Phys. Rev. Lett. **91**, 137202 (2003).
[10] U. K. Rößler, Phys. Rev. B **59**, 13577 (1999).
[11] A. Perumal, V. Srinivas, V. V. Rao, and R. A. Dunlap, Physica B **292**, 164 (2000).
[12] A. B. Harris, J. Phys. C **7**, 1671 (1974).
[13] C. V. Mohan and H. Kronmüller, J. Magn. Magn. Mater. **182**, 287 (1998).
[14] D. R. Denholm and T. J. Sluckin, Phys. Rev. B **48**, 901 (1993).
[15] Z. Ristivojevic, Phys. Rev. B **80**, 174528 (2009).
[16] T. Hase, H. Raanaei, H. Lidbaum, C. Sánchez-Hanke, S. Wilkins, K. Leifer, and B. Hjörvarsson, Phys. Rev. B **80**, 134402 (2009).
[17] M. Björck and G. Andersson, J. Appl. Crystallogr. **40**, 1174 (2007).
[18] M. Pärnaste, M. van Kampen, R. Brucas, and B. Hjörvarsson, Phys. Rev. B **71**, 104426 (2005).
[19] S. Bramwell, P. Holdsworth, and M. Hutchings, J. Phys. Soc. Jpn. **64**, 3066 (1995).
[20] J. Als-Nielsen, S. T. Bramwell, M. T. Hutchings, G. J. McIntyre, and D. Visser, J. Phys. Condens. Matter **5**, 7871 (1993).
[21] H. Rønnow, A. Wildes, and S. Bramwell, Physica B **276–278**, 676 (2000).
[22] H. J. Elmers, J. Hauschild, and U. Gradmann, Phys. Rev. B **54**, 15224 (1996).
[23] A. Taroni, S. Bramwell, and P. Holdsworth, J. Phys. Condens. Matter **20**, 275233 (2008).
[24] L. Onsager, Phys. Rev. **65**, 117 (1944).
[25] M. Campostrini, M. Hasenbusch, A. Pelissetto, P. Rossi, and E. Vicari, Phys. Rev. B **65**, 144520 (2002).
[26] N. Saito, H. Hiroyoshi, K. Fukamichi, and Y. Nakagawa, J. Phys. F **16**, 911 (1986).
[27] E. Babic, K. Zadro, Z. Marohnic, D. Drobac, and J. Ivkov, J. Magn. Magn. Mater. **45**, 113 (1984).
[28] P. Gaunt, S. C. Ho, G. Williams, and R. W. Cochrane, Phys. Rev. B **23**, 251 (1981).
[29] Y. Yeshurun, M. B. Salamon, K. V. Rao, and H. S. Chen, Phys. Rev. B **24**, 1536 (1981).
[30] C. Sankar, S. Vijayanand, and P. Joy, Solid State Sci. **11**, 714 (2009).
[31] P. Archambault, S. T. Bramwell, and P. C. W. Holdsworth, J. Phys. A: Math. Gen. **30**, 8363 (1997).
[32] M. Hasenbusch, K. Pinn, and S. Vinti, Phys. Rev. B **59**, 11471 (1999).
[33] Z. Q. Qiu, J. Pearson, and S. D. Bader, Phys. Rev. Lett. **70**, 1006 (1993).
[34] C. M. Schneider, P. Bressler, P. Schuster, J. Kirschner, J. J. de Miguel, and R. Miranda, Phys. Rev. Lett. **64**, 1059 (1990).
[35] R. Zhang and R. F. Willis, Phys. Rev. Lett. **86**, 2665 (2001).
[36] H. Lidbaum, *Transmission Electron Microscopy for Characterization of Structures, Interfaces and Magnetic Moments in Magnetic Thin Films and Multilayers*, PhD. thesis, Uppsala University, 2009.
[37] B.-G. Shen, L.-Y. Yang, L. Cao, and H.-Q. Guo, J. Appl. Phys. **73**, 5932 (1993).
[38] T. S. Bramfeld and R. F. Willis, J. Appl. Phys. **103**, 07C718 (2008).
[39] Z. Q. Qiu, J. Pearson, and S. D. Bader, Phys. Rev. Lett. **67**, 1646 (1991).
[40] S. Blundell, *Magnetism in Condensed Matter* (Oxford University Press, Oxford, 2001).